

# On the characterisation of solar cells using light beam induced current measurements

L.J Bezuidenhout, E.E van Dyk, F.J Vorster and MC du Plessis

Nelson Mandela Metropolitan University

Centre for Energy Research

## Abstract

The Light Beam Induced Current (LBIC) measurement technique is used to perform localized characterization on solar cells using a light beam as a probe. This technique allows the determination of the local photo-response of a solar cell which enables characterization of the spatial distribution of defects and electrical parameters. By scanning the beam probe across a solar cell while measuring the current-voltage characteristics at each point, a map of various cell parameters such as short-circuit current, carrier lifetime, quantum efficiency of a solar cell and other device parameters may be extracted using this technique.

In this study a high resolution LBIC system was designed and constructed. This paper discusses the design of the LBIC system, the software interfacing of the data acquisition system, local photo-response of the individual cells and LBIC maps indicating areas of reduced efficiency or performance as a function of spatial distribution within different solar cell technologies, including, single-crystalline (*c-Si*) and multicrystalline (*mc-Si*) Silicon. In addition this paper also discusses the basic principle of the parameter extraction algorithm used to extract device parameters of a solar cell.

*Keywords:* parameter extraction, LBIC, device parameters, photo-response, I-V characteristics

## 1. Introduction

The semiconductor materials used to manufacture solar cells are not always defect free and the defects present in the bulk and surface of these materials negatively impact the electrical performance of the solar cells. Standard characterisation tools, such as visual inspection, electroluminescence and infrared imaging act as complimentary techniques to characterise the extent of these performance limiting defects. LBIC is a non-destructive technique that focuses light onto a solar cell device thus creating a photo-generated current that can be measured as a function of its position on the cell surface. By measuring the variation in the photo generated current as the beam probe is scanned across the cell, the performance limiting defects can be identified and therefore characterised.

To determine the device parameters such as the parasitic resistances, diode ideality factor and saturated current of the photovoltaic devices a parameter extraction routine was developed. The routine is based on the principle of minimizing the area under the I-V curve from the experimental data collected and the model of the diode equation based on a set of initial guesses for each parameter. The parameters extracted allow for the characterisation of the defects present in the solar cells.

### 1.1. Objectives

The objective of this investigation is to design and construct an LBIC system to identify performance degrading defects in solar cells. The primary aim is to create a device parameter extraction routine that best approximates the parameters. By extracting these device parameters the solar cell can be electrically characterised and thus the performance of the device can be improved.

### 2. Proposed model or Conceptual method

A solar cell consists of a semiconductor diode, which is formed by joining n-type and p-type semiconducting materials. Semiconducting solar cells are generally represented by the one-diode or two-diode equivalent models as shown in figure 1.

The I-V characteristic of a solar cell is described by the two diode equation (Thantasha, N. 2010).

$$I = I_L - I_{01} \exp\left(\frac{qV}{n_1 kT}\right) - I_{02} \exp\left(\frac{qV}{n_2 kT}\right) - \frac{V}{R_{sh}} \quad \text{.....1}$$

Where  $I_{01}$  is the ideal saturated current,  $I_{02}$  is the non-ideal saturated current,  $n_1$  and  $n_2$  the diode ideality factors,  $I_L$  the illuminated current and  $T$  the temperature.

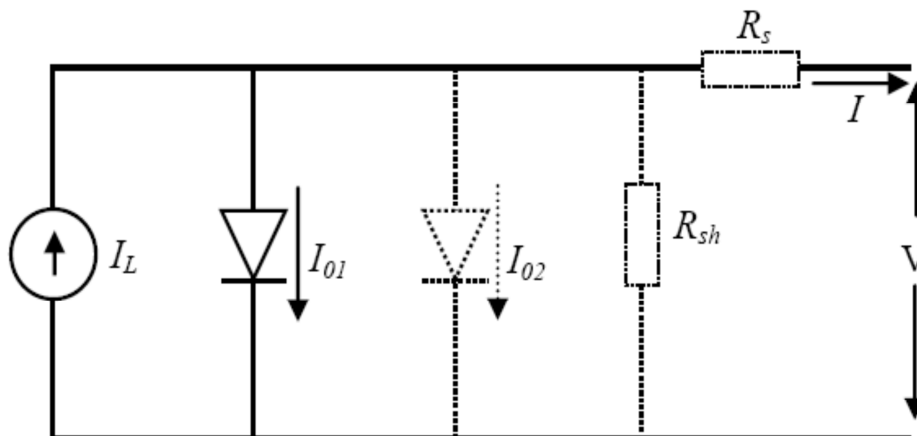
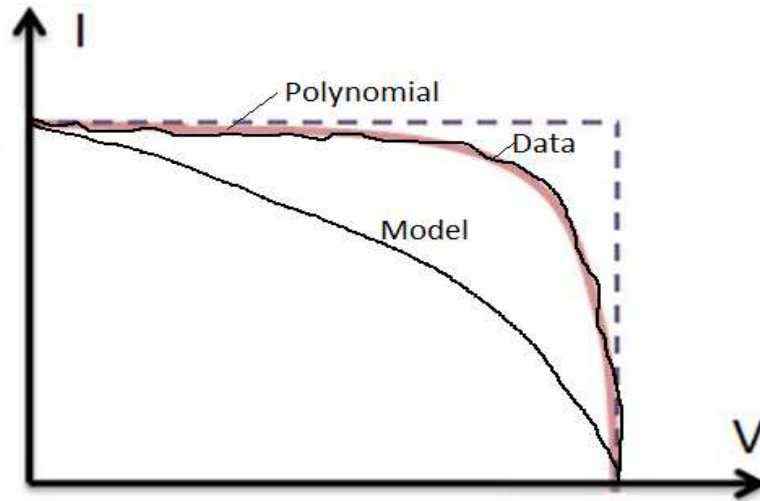


Figure 1: Equivalent cell model (Macabebe, E. 2009)

When the semiconducting diode in the solar cell is subjected to light, the incoming photons that have enough energy will excite the electrons from the valence band to the conduction band leaving holes in the valence band. In the region of the junction an electric field will sweep the excess electrons to the n side of the junction, resulting in an excess of charge and thus an open circuit voltage ( $V_{oc}$ ) can be measured. The short-circuit current ( $I_{sc}$ ) is a function of the concentration of excited charge carriers which is related to the incident intensity of the light.

To accurately explain the I-V characteristics of a photovoltaic module the resistance due to defects of the cell  $R_{sh}$  and the series resistance  $R_s$  cannot be ignored as series resistance reduces the voltage produced by the cell, which then reduces the performance of the solar cell. The shunt resistance due to crystal impurities which produces shunt paths (Gxasheka, A. 2008), giving rise to shunt currents ( $I_{sh}$ ), that lead current away current from their intended direction and therefore decreasing the performance of the cells. For a good solar cell  $R_{sh}$  must be infinitely large and therefore  $I_{sh}$  negligible.

The solar cell device performance is described in terms of the parameters derived from the light I-V curve shown in figure 2. The extraction routine used to obtain these device parameters makes use of the area between the I-V curve from the measured data set and the diode equation modelled with initial guesses for each parameter that lies within the theoretical range.



**Figure 2: Light I-V characteristics of a solar cell**

The proposed model minimizes the area under the curve between the I-V curve obtained from the data and the model. Since the raw data is piece-wise smooth, which makes integration over such a region very difficult, an  $n^{\text{th}}$  degree polynomial was created using the least-square fit method that accurately fits the experimental I-V data and thus making integration simpler. By keeping one parameter fixed at a time and using the initial guesses for the other parameters we integrate over the area between the polynomial and the model, where the initial guesses are updated by the values obtained from the model each time.

To minimize the area under the curve with respect to each parameter, the best fit model was obtained by setting the derivative of the resulting integral to zero, thus,

$$\frac{dI}{dx} = 0 \quad \text{where } x = [n, R_s, R_{sh}, I_0, I_L] \quad \dots\dots\dots 2$$

To iteratively solve this equation Newton's method was used to determine the roots of equation 2. The method takes advantage of the ratio between the function and small changes to the solution as  $I$  changes with respect to each parameter and is given by equation 3.

$$X_{x_0} = x_0 - \frac{I(x_0)}{I'(x_0)} \quad \dots\dots\dots 3$$

The method yields a good approximation for  $n$ ,  $I_0$ , and  $R_s$ , however, problems occur with  $I_L$  and  $R_{sh}$ . Integrating the diode equation and taking the derivative with respect to each parameter,  $I_L$  goes to zero and  $R_{sh}$  goes to infinity. Infinitely large values for  $R_{sh}$  are expected for the ideal case. Another method was thus required to determine these last two parameters.

$I_L$  was approximated to be  $I_{sc}$ , which is a good approximation since all the other parameters at that point are negligible. For  $R_{sh}$  a set of values that surrounds the theoretical value was chosen. By using the other parameters obtained from the model and plotting all the values of

the set for the diode equation, the value that gives the best fit to the polynomial from the set was chosen.

### 3. Research methodology

The LBIC system designed for this project consist of a laser source for current generation in the cells at a point, beam expander, aperture, objective lens and x-y stage driven by stepper motors as indicated in figure 3. The adjustable aperture in front of the objective lens allows the user to vary the beam diameter incident on the sample. A Labview programme was written to interface the data acquisition systems and the x-y stages. The flowchart illustrating the sequence of the procedure within the Labview algorithm is given by figure 4.

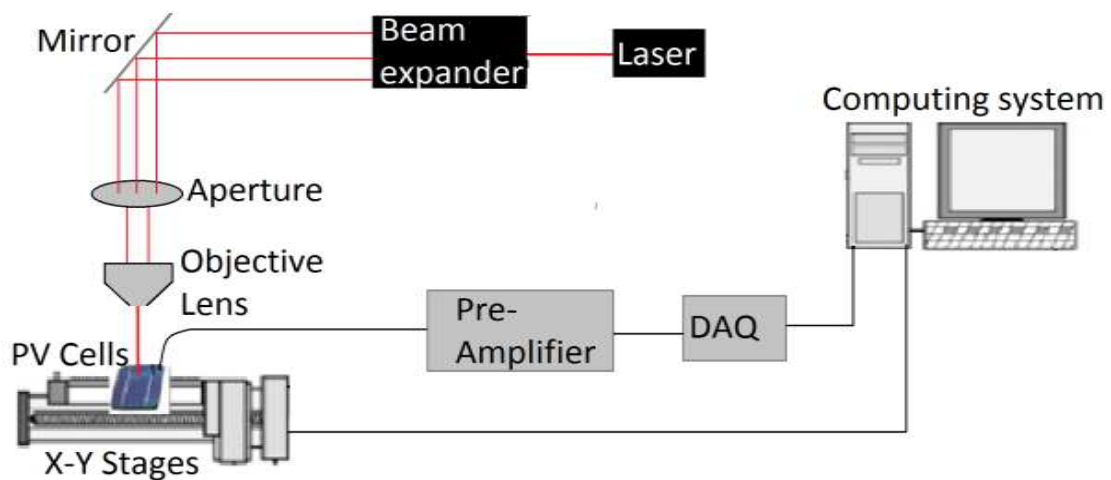


Figure 3: Schematic of LBIC system

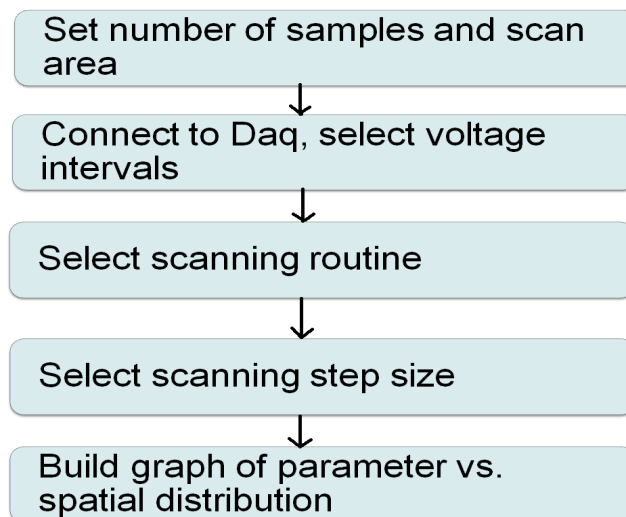


Figure 4: Flowchart illustrating Labview algorithm

By scanning the beam across the solar cell in a raster pattern while measuring photo-generated current as a function of spatial distribution, a structural image of the current across the cell is mapped and regions of current reducing defects can be identified.

In addition, the system allows for forward and reverse biasing of the sample using an alternating current voltage source (waveform generator). At predetermined bias-voltages the photo-generated current is measured which allows for I-V characterisation of the cell and subsequent device parameter extraction.

#### 4. Results

Single crystalline and multi-crystalline Silicon solar cells were used for analysis. The LBIC measurements were done using a 633 nm wavelength laser beam with a spot size of approximately 100  $\mu\text{m}$  incident on the cell and 100  $\mu\text{m}$  step size. Figure 5 shows an  $I_{sc}$  map of a single crystalline silicon solar cell. The scan shows clearly the contact fingers and other current reducing features. The fingers acts as shading features and therefore no current is generated (Thantasha, N. 2010). The scan indicates a scratch across the solar cell; this is due to poor handling of the cell. Figure 6 indicates a higher resolution LBIC scan of the circled area in figure 5. This current reducing defect could be due to impurities present in the semiconductor material that could have been introduced during the manufacturing processes.

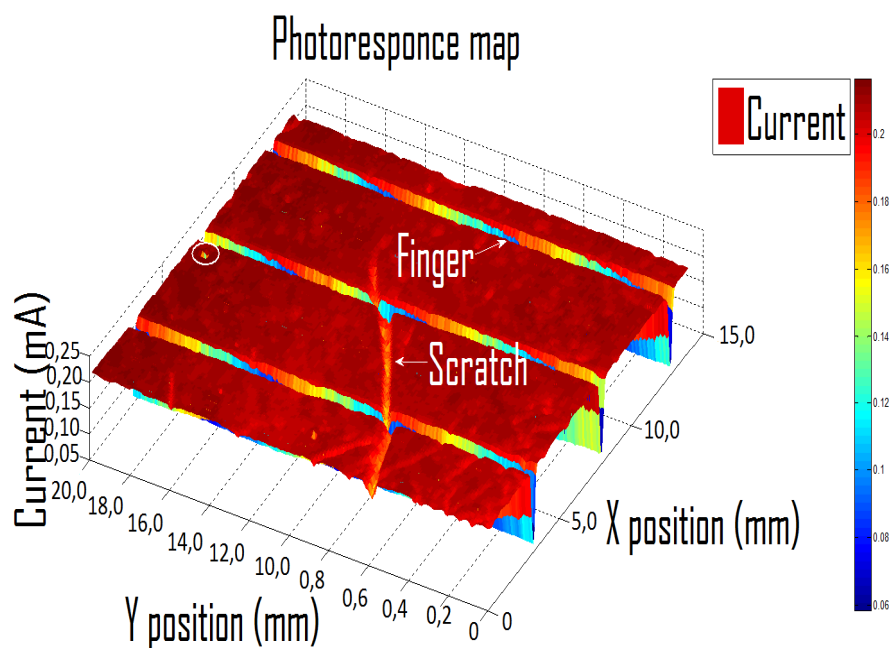
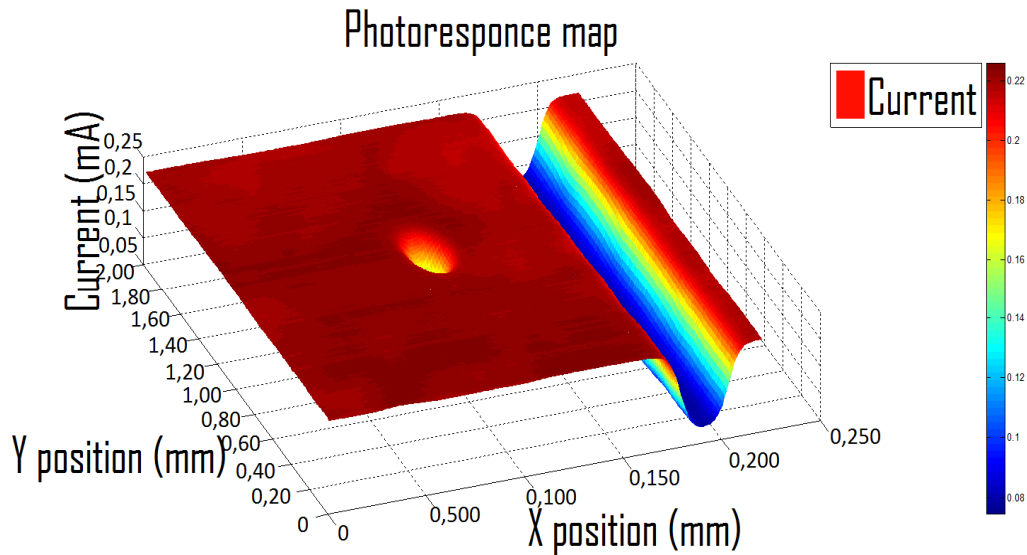
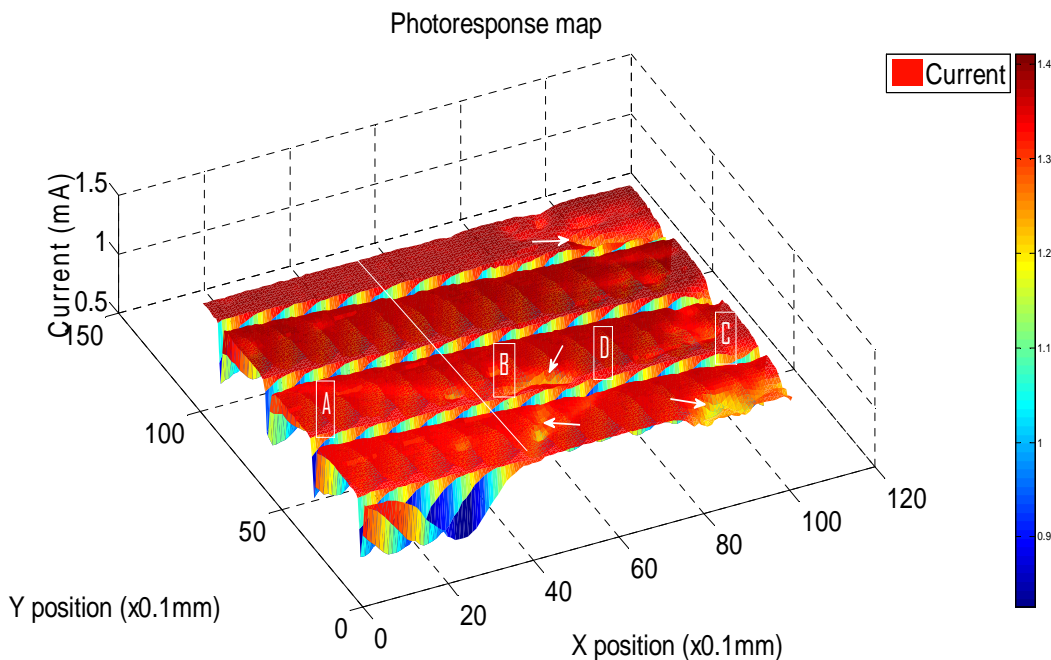


Figure 5: LBIC map of cell area 15.0x20.0  $\text{mm}^2$  at zero biasing voltage.



**Figure 6: LBIC map of circled area at zero biasing voltage.**

Figure 7 shows a LBIC map of the 10.0 mm x 10.0 mm multi-crystalline Si solar cell used in this study. The LBIC scan was done with a 633 nm laser beam with a spot size of approximately 150  $\mu\text{m}$  spot size and 100  $\mu\text{m}$  step sizes. Since relatively low resolutions were used for the LBIC mapping, grain boundaries were not clearly defined. The regions indicated by the arrows show areas of defects within the cell, some of the regions could be grain boundaries or defects within the semiconductor material presented in the process of manufacturing the cells.



**Figure 7: LBIC map of a multi-crystalline Si cell, indicating regions where line scans and I-V measurements were taken**

By scanning the light beam across one axis and keeping the other axis constant a line scan across the multi-crystalline Si solar cell was obtained at different biasing voltages as shown in figure 8. The figure clearly shows the current drop due to the metallized shading of the contact fingers of the cell. The lines present below  $I_{sc}$  represent the scan taken at reverse

bias voltages while the lines above indicate scans taken at forward bias voltages. The extent of the current reducing defects and their effect on the photo generated current at different biasing voltages can clearly be seen by figure 8.

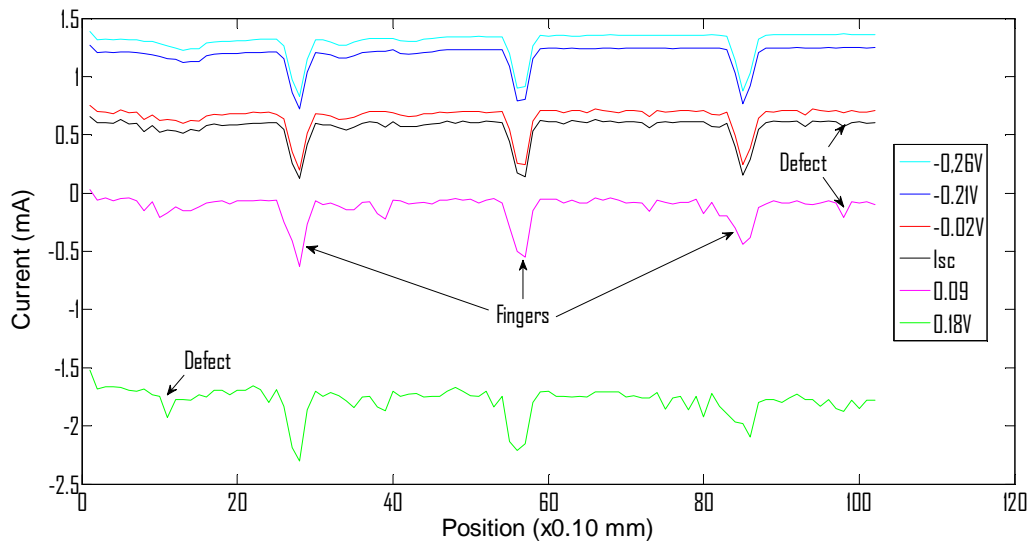


**Figure 8: Line scans cross the multi-crystalline Si solar cells at different biasing voltages**

Figure 9 shows the I-V curves of the points indicated on the multi-crystalline solar cell in figure 7, and will be used to extract the cell parameters at these points on the cell. The data points from the I-V curve were used to obtain the device parameters by using the method described. Parameters such as diode ideality factor ( $n$ ), series resistance ( $R_s$ ), shunt resistance ( $R_{sh}$ ), saturated current ( $I_0$ ) and the illuminated current were extracted and are listed in table 1. From figure 9 the small differences in the I-V characteristics of the points on the cell can be seen. Points A and D shows slightly better current yields than regions B and C and this is due to the smaller shunt currents at these regions.

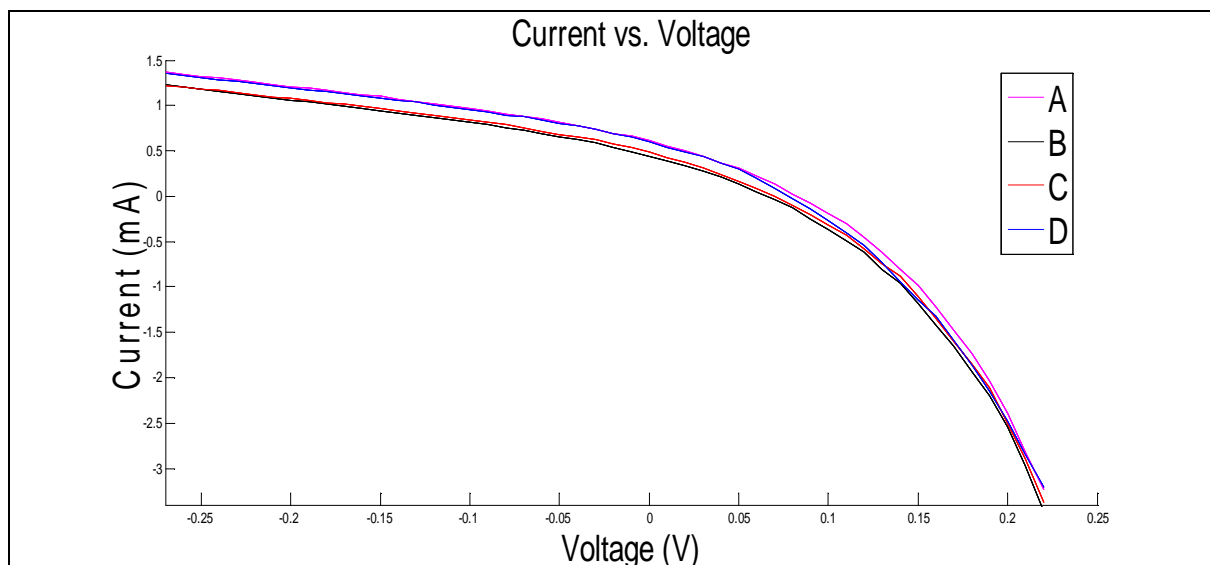


**Figure 9: I-V curve of the points A, B, C, and D indicated on figure 7**

**Table 1: Device performance parameters of a multi-crystalline Si solar cell.**

Region	$I_L$ (mA)	n	$R_{sh}$ ( $\Omega$ )	$R_s$ ( $\Omega$ )	$I_0$ (mA)
A	1.3501	1.975	55.84	2.371	$9.00 \times 10^{-4}$
B	1.3675	1.820	49.53	1.661	$8.96 \times 10^{-4}$
C	1.2267	1.797	45.90	3.034	$8.93 \times 10^{-4}$
D	1.2221	1.985	60.69	2.863	$8.98 \times 10^{-4}$

The lower voltage region of the I-V curves are influenced by  $R_{sh}$  and the higher voltage region by  $R_s$ . Table 1 shows that these values differ slightly and this could be due to different inter-grain defects present at these regions, which reduce photo-generated current (Gxasheka, A. 2008). The lower  $R_{sh}$  value is indicative of an increase of shunt paths across the p-n junction of the cell, which leads the photo-generated current away from its proposed direction, thus we expect the performance of regions B and C to be less than regions A and D. The device parameters  $I_L$ , n and  $I_0$  are also listed in the table, these have fairly similar values for all the regions.

## 5. Conclusions and recommendations

The defects present in the semiconductor materials, mainly due to impurities that occur during the manufacturing process reduce the performance of the solar cells and it is therefore important to be able to detect these defects. LBIC is a non-destructive method that allows for the identification and characterisation of the defects present in the solar cells. The LBIC system that is being developed is able to map the photo-generated current as a function of position on the cell. By observing this current distribution map, defect regions in the cells may be identified. The single and multi-crystalline Si solar cells showed regions of current reducing defects that ultimately reduce the performance of the solar cell. In addition, the LBIC system is able to measure the I-V characteristics at each point on the solar cell, which allowed for the extraction of the device performance parameters at each measurement point. The parameters obtained from the multi-crystalline Si cell were used to describe the performance of the cell at various regions. Future work involves extracting parameters over the entire cell and mapping these parameters as a function of position for a better understanding of the performance of the solar cell.

## References

1. Thantasha, N. (2010). *Spatially Resolved Opto-Electric Measurement of Photovoltaic materials and devices*, A Thesis Submitted in partial fulfillment of the Requirements of Philosophiae Doctor in the Faculty of Science at Nelson Mandela Metropolitan University. Port Elizabeth: Nelson Mandela Metropolitan University.
2. Gxasheka, A. (2008) *On the optical characterisation of photovoltaic devices*. A Thesis Submitted in partial fulfillment of the Requirements of Philosophiae Doctor in



the Faculty of Science at Nelson Mandela Metropolitan University. Port Elizabeth: Nelson Mandela Metropolitan University.

3. Munji, M. (2011) *Characterisation of concentrator solar cells devices and materials using light beam induced current measurements.* A Thesis Submitted in partial fulfillment of the Requirements of Philosophiae Doctor in the Faculty of Science at Nelson Mandela Metropolitan University. Port Elizabeth: Nelson Mandela Metropolitan University.
4. Macabebe, E. (2009) *Investigation of device and performance parameters of photovoltaic devices.* A Thesis Submitted in partial fulfillment of the Requirements of Philosophiae Doctor in the Faculty of Science at Nelson Mandela Metropolitan University. Port Elizabeth: Nelson Mandela Metropolitan University.